

# Model-Driven Based Deep Unfolding Equalizer for Underwater Acoustic OFDM Communications

Cui Yang, Yalu Xu, Hao Zhao, Yankun Chen and Fei Ji

**Abstract**—It is a challenge to design a equalizer for complex time-frequency doubly-spread channels. In this paper, we employ the deep learning (DL) architecture by that unfolding an existing iterative algorithm to build an equalizer named underwater deep network (UDNet) for underwater acoustic (UWA) orthogonal frequency division multiplexing (OFDM) signal. Considering constellation recognition is a classification issue, the one-hot coding and softmax layer are adopted in the proposed network to achieve the minimum Kullback-Leibler (KL) criterion. Simultaneously, we introduce a sliding structure based on the banded approximation of the channel matrix to reduce computational complexity and aid UDNet performs well for different length signals without changing the network structure. Furthermore, we apply the environment of the true UWA channel as much as possible, including utilize measured doubly-spread UWA channel and offshore background noise to evaluate the UDNet. Experimental results show that in the case of 10-35dB SNR, UDNet achieves better performance with low computational complexity.

**Index Terms**—Underwater acoustic communication, OFDM, deep learning, frequency domain equalization, unfolding network

## I. INTRODUCTION

In underwater environments, acoustic waves experience lower attenuation than electromagnetic waves and lower scattering that light waves experience in such environment [1]. Therefore, Underwater acoustic (UWA) communication is the most effective way to achieve information exchange. However, UWA faces some difficulties, compared with the wireless communications, such as the frequency-dependent attenuation, the time-varying multipath, and the severe Doppler effect, e. g [2]–[4]. So far, UWA communication is generally recognized as one of the most challenging communication media, because of its doubly-spread characteristic [5]. Moreover, the UWA channel is rich in interference, such as interference from sonar operations, marine mammals, shrimp snapping noise, and malicious jamming [6]. These characteristics have brought obstacles to the high-rate communication of UWA [7]. Orthogonal frequency division multiplexing (OFDM) as one of the multi-carrier modulation techniques has been proved to be a viable option for dealing with the long-delay multi-path UWA channels [8], [9]. It has shown robustness against underwater inter-symbol interference (ISI) [10]. However, inter-carrier interference (ICI) caused by doubly-spread channel will degrades the performance of OFDM, especially for a large number of sub-carriers and the high order constellation, which are practical as in UWA communication [11]. Furthermore, the UWA channel is wideband in nature due to the small ratio of the carrier frequency to the signal bandwidth which cause frequency-dependent Doppler shifts. It renders existing ICI

reduction techniques ineffective [12]. That is because classical interference cancellation methods such as zero-forcing (ZF), minimum mean squared error (MMSE) equalizers are usually based on the assumption that ICI happens in very limited number of sub-carriers [13]. But the actual UWA channel matrix exists a great quantity of ICI. Therefore, performance of those classical equalizers degrades significantly while facing ill-conditioned channel matrix caused by Doppler shift.

In recent years, DL methods have achieved several excellent results in the field of communications. In particular, DL has different applications, such as signal estimation, modulation recognition and equalization. Ye first attempts to utilize an end-to-end OFDM receiver fully connected deep neural network (FC-DNN) that replace channel estimation, signal detection and demodulation modules jointly based the DNN network [14]. The drawback of FC-DNN is that DL-receiver treats itself as a black box, which leads to the data-driven method unexplainable and unpredictable. To solve these issues, a model-driven DL-receiver, called ComNet was proposed, which combine expert knowledge of communication algorithms and exhibits higher data recovery accuracy than FC-DNN [15]. In the field of UWA signal processing, a DL-based receiver was designed for single-carrier communications over time-varying UWA channels. It works with online training and test modes for accommodating the time variability of UWA channels [16]. Aiming to improve the OFDM communication performance over UWA doubly-selective channels, a novel architecture named DECCN is proposed, which based on convolutional neural network (CNN) to compose an encoder and a decode [17]. Compared with the integrated design, the method of using DL network to replace a certain signal processing module has also achieved good performance. In order to improve the problem that the modulation recognition performance in multipath fading channels could be seriously degraded especially for high-order quadrature amplitude modulation (QAM) signals, a blind equalization-aided DL approach proposed that DL network as a recognizer module to recognize QAM signals in the presence of multi-path propagation [18]. It achieve a better performance than the conventional DL modulation recognition approaches, and it is robust to the multipath number deviation which might happen in practice. So as to refine the DNN output for improved equalization accuracy, a new turbo equalizer first try to adopt DNN in the framework of bit-interleaved coded modulation iterative demodulation, which can accelerate decoding convergence to achieve a significant gain [19]. In addition to using classic DL networks, a promising approach to designing

deep architectures is by unfolding existing computationally complex iterative algorithms [20]. Each iteration is treated as a layer and the algorithm is called the network. The learning begins with the existing algorithm as an initial starting point and use optimization methods to improve the algorithm [21]. Therefore, based on the current maximum likelihood (ML) algorithm model and deep unfolding method, the detector network (DetNet) is constructed for multi-input multi-output (MIMO) detection [21]. The MIMO scenario studied by DetNet is relatively simple that might induce several performance degradation in practice. Moreover, a novel sliding cascaded network (SCN) is designed for large Doppler frequency shift channels [13]. SCN designs loss function follows minimum mean square error (MSE) criterion and regression idea. In general, the model-driven deep unfolding method achieves better performance in signal equalization comparing with the existing traditional methods [13], [21]. The complexity of the UWA channel makes equalization issue more important, meanwhile, the integrated design has high requirements for data matching. Furthermore, as the data rate increases, the delay spread becomes more pronounced, greatly increasing computational complexity of conventional time-domain multi-channel equalization [22], [23]. Considering the above issues, the frequency domain equalization problem is analyzed in this paper.

Compare with existing works, our main contributions are summarized as:

- In order to solve the problem of frequency domain signal detection in complex UWA-OFDM systems, we propose a DL network architecture called UDNet. Considering that constellation recognition as a classification issue, one-hot coding and classification structure are applied to UDNet. These improvement measures result in the soft output of the network being the probability. So as to make the training effect of the UDNet better, we adopt the minimum KL criterion, rather than the previous network employ MSE criterion. Additionally, more cross-layer residual connections are introduced to improve network capability. We show that UDNet obtains accuracy better than that of the decoder such as semidefinite relaxation equalizer, the decision feedback equalizer, with acceptable computational complexity.
- In contrast of integrated design requires multiple training for different channel models, UDNet performs a single training with a single SNR and can adapt to different models with multiple SNR. Moreover, we apply a sliding structure that assist UDNet adapt some length signals without modifying the network architecture. Thus, the proposed network can handle received signals of different sub-carriers to increase practicability.
- In order to make the experimental results more persuasive, we utilize the environment of the true UWA channel as much as possible. Such as we adapt measured UWA channel models and the additive offshore noise measured in Yangjiang to evaluate our network. Experimental re-

sults show that with various scenarios, UDNet achieves good equalization performance with low computational complexity.

The structure of this paper is as follows. In the section II, the doubly-spread UWA channel models are established, including under perfect channel State Information (CSI) and imperfect CSI. In the section III, the proposed equalizer network structure introduced in detail. In the section IV, we provide the experimental parameters of the network training and the performance of the proposed network in different channels models. Moreover, our network tested with the true offshore background noise. The final section makes the conclusion of the paper.

**Notation:** In this paper, we define the normal distribution which mean value is  $\bar{u}$  and standard deviation is  $\sigma$  as  $\mathcal{N}(\bar{u}, \sigma)$ . We utilize Boldface uppercase letters represent matrices and boldface lowercase letters represent vectors. The superscript  $(\cdot)^T$  means the transpose. The  $i^{th}$  element of the vector  $\mathbf{s}$  will be denoted as  $\mathbf{s}_i$ . The  $\Re(\cdot)$  represents the real part and the  $\Im(\cdot)$  represents the imaginary part when considering a complex vector or matrix.

## II. SYSTEM MODEL

### A. UWA-OFDM System Structure

We construct a single input single output (SISO) UWA-OFDM system, and the proposed system architecture with DL based signal equalization is described in Fig. 1. At the transmitter, the input bits of UWA-OFDM system are mapped into a digital modulation to gain  $S(k)$  where represents the transmitted signal on the  $k^{th}$  sub-carrier. Then, the transmitted data streams  $S(k)$  is converted to the time domain after  $N$ -point inverse fast Fourier transform (IFFT) transform, this process can be expressed as

$$s(n) = \frac{1}{N} \sum_{n=0}^{N-1} S(k) e^{-j \frac{2\pi}{N} nk}, \quad (1)$$

where  $s(n)$  means the  $n^{th}$  time sample in a OFDM symbol with  $N$  sub-carriers. Later,  $s(n)$  is arranged into blocks by a parallel-to-serial (P/S) converter. And a cyclic prefix (CP) is then adopted. We assume that the CP can cancel the maximum delay interference in the channel, so that ISI can be ignored. We can study the ICI in a frame of data. The multipath effects lead to channel time spread, multiple Doppler-scaling paths and time variation of the UWA channel lead to Doppler spread, so that UWA communication channel is doubly-spread [24]. Given the received signal  $y(n)$  which after the transmitted signal  $s(n)$  through the channel  $h(n, l)$  can be expressed as

$$y(n) = \sum_{n=0}^{N-1} \sum_{l=0}^{L-1} h(n, l) s(n - l) + z(n), \quad (2)$$

where  $h(n, l)$  means the doubly-spread complex gain of the  $l^{th}$  path at the  $n^{th}$  moment,  $L$  means represents the total number of signal transmission paths, and  $z(n)$  represents additive white gaussian noise (AWGN).

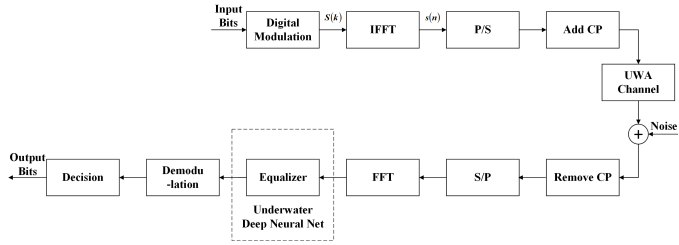


Fig. 1: UWA-OFDM system with DL based signal equalization.

At the receiver, the received signal need to remove the CP and through the serial-to-parallel (S/P) conversion module. Then, the received signal is performed discrete Fourier transform (DFT). The vector  $\mathbf{y} = \mathcal{F}(y)$  represents received signal  $y(n)$  is subjected to DFT processing.

The doubly-spread UWA channel can be expressed in frequency domain as:

$$\mathbf{H} = \begin{bmatrix} H_{00} & H_{(N-1)1} & \cdots & H_{2(N-2)} & H_{1(N-1)} \\ H_{10} & H_{01} & \cdots & H_{3(N-2)} & H_{2(N-1)} \\ \vdots & \vdots & \ddots & \vdots & \vdots \\ H_{(N-2)0} & H_{(N-3)1} & \cdots & H_{0(N-2)} & H_{(N-1)(N-1)} \\ H_{(N-1)0} & H_{(N-2)1} & \cdots & H_{1(N-2)} & H_{0(N-1)} \end{bmatrix}. \quad (3)$$

where  $\mathbf{H} = 2\mathcal{D}\mathcal{F}(h)$  represents the time-domain channel matrix after two-dimensional DFT (2D-DFT) and  $\mathbf{H} \in \mathbb{E}^{N \times N}$ .  $\mathbf{H}$  reflects the mutual interference between sub-carriers. As Fig. 2 shows that for a quasi-static channel heatmap, the energy of the frequency-domain channel matrix is concentrated only on the diagonal of the matrix, and as it comes to a doubly-spread channel heatmap, the amplitude of each coefficient in the channel matrix changes smoothly along the banded area of the propagation matrix. Therefore, the signal transmission process can be modeled as

$$\mathbf{y} = \mathbf{H}\mathbf{s} + \mathbf{z}, \quad (4)$$

where received vector  $\mathbf{y} = \mathcal{F}(y)$  represents the received signal in frequency domain and  $\mathbf{y} \in \mathbb{E}^N$ , transmitted vector  $\mathbf{s} = \mathcal{F}(s)$  means the transmitted signal in frequency domain and  $\mathbf{s} \in \mathbb{C}^N$  is the transmitted vector of the symbols from several limit constellation  $\mathbb{C}$ , noise vector  $\mathbf{z} = \mathcal{F}(z)$  means the noise with size  $N$  in frequency domain. The obtained received vector  $\mathbf{y}$  and the estimated channel  $\mathbf{H}$  can be equalized with UDNet to get the transmission signal constellation prediction value. The output bits can be gained through the demodulation and decision modules.

### B. Imperfect CSI of Channel

There are random interference factors such as the attenuation of information energy and waveform distortion caused by the nonlinearity of the system in the UWA channel [25]. Thus, it is difficult to obtain perfect CSI in practical UWA communication systems. In order to evaluate the robustness of the proposed network in practice, we define a random error matrix  $\mathbf{U}$  to simulate imperfect CSI.

According to Eq. (2), when the CSI is imperfect, the relationship between the transmitted signal and the received signal can be derived as

$$y(n) = \sum_{l=0}^{L-1} u(n, l)h(n, l)s(n-l) + z(n), \quad (5)$$

where  $u(n, l)$  represents the random error factor of the  $l^{th}$  path at the  $n^{th}$  moment.

According to Eq. (4), we can obtain the expression in frequency domain

$$\mathbf{y} = \mathbf{U}\mathbf{H}\mathbf{s} + \mathbf{z}, \quad (6)$$

where

$$\mathbf{UH} = \begin{bmatrix} U_{00}H_{00} & \cdots & U_{1(N-1)}H_{1(N-1)} \\ U_{10}H_{10} & \cdots & U_{2(N-1)}H_{2(N-1)} \\ \vdots & \ddots & \vdots \\ U_{(N-2)0}H_{(N-2)0} & \cdots & U_{(N-1)(N-1)}H_{(N-1)(N-1)} \\ U_{(N-1)0}H_{(N-1)0} & \cdots & U_{0(N-1)}H_{0(N-1)} \end{bmatrix}. \quad (7)$$

The random error matrix  $\mathbf{U}$  which with mean value is  $\bar{u}$  and standard deviation is  $\sigma$ , which each of its elements is generated from the normal distribution  $\mathcal{N}(\bar{u}, \sigma)$ . In the perfect CSI model,  $\mathbf{U}$  is treated as an all-ones matrix.

## III. UNDERWATER DEEP NETWORK

In this section, we elaborate on the network structure of UDNet. Traditional equalization algorithms can cancel ICI when its occurrence in a very limited number of subcarriers. However, the UWA channel matrix has a large amount of ICI due to its doubly-spread characteristics. Therefore, we construct UDNet based on model-driven deep unfolding network to improve equalization performance. Fig. 3 shows a single layer network of UDNet with classification structure.

### A. Data Pre-processing

The input complex signals of UDNet are split into imaginary parts and real parts:

$$\mathbf{y} = \begin{bmatrix} \Re(\mathbf{y}) \\ \Im(\mathbf{y}) \end{bmatrix}, \mathbf{s} = \begin{bmatrix} \Re(\mathbf{s}) \\ \Im(\mathbf{s}) \end{bmatrix}, \quad (8)$$

$$\mathbf{z} = \begin{bmatrix} \Re(\mathbf{z}) \\ \Im(\mathbf{z}) \end{bmatrix}, \mathbf{H} = \begin{bmatrix} \Re(\mathbf{H}) & -\Im(\mathbf{H}) \\ \Im(\mathbf{H}) & \Re(\mathbf{H}) \end{bmatrix}, \quad (9)$$

where received vector  $\mathbf{y} \in \mathbb{E}^{2N}$ , channel matrix  $\mathbf{H} \in \mathbb{E}^{2N \times 2N}$  and transmitted vector  $\mathbf{s} \in \hat{\mathbb{C}}^{2N}$  where  $\hat{\mathbb{C}} = \Re\{\mathbb{C}\}$ .

We implement digital modulation on the transmitted OFDM signal and then perform one-hot encoding of the reparameterized discrete modulated signal constellation  $\hat{\mathbb{C}} = \{c_1, \dots, c_{|\hat{\mathbb{C}}|}\}$ . For each possible  $c_i$ , we arrange a unit vector  $\mathbf{p}_i \in \mathbb{E}^{|\hat{\mathbb{C}}|}$ . We define the mapping function  $c = \varepsilon_o(\mathbf{p})$  that  $c_i = \varepsilon_o(\mathbf{p}_i)$  for  $i = 1, \dots, |\hat{\mathbb{C}}|$ . For example, the real part of

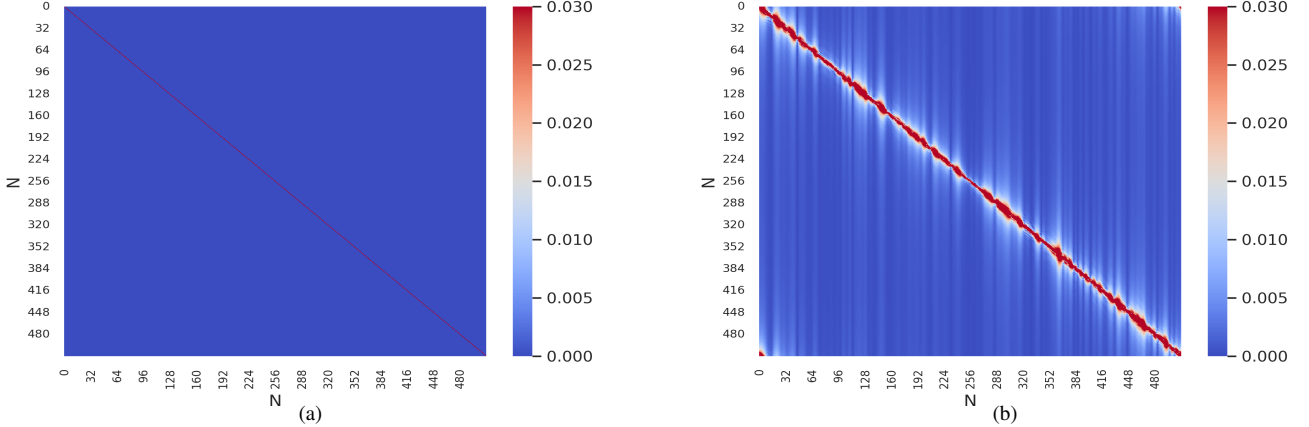


Fig. 2: Heatmap of baseband equivalent channel matrix with subcarrier number  $N = 512$  in frequency domain: a) quasi-static channel heatmap b) doubly-spread channel heatmap.

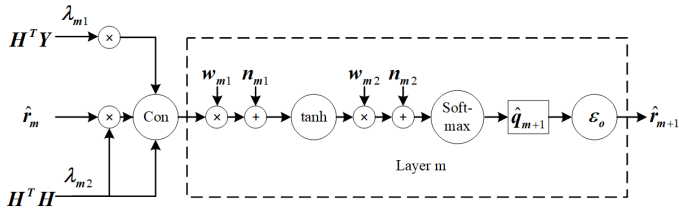


Fig. 3: A flowchart of the  $m^{\text{th}}$  layer of UDNet with classification structure. The network consists of  $M$  layers, where the output of each layer is the input to the next layer.

the quadrature phase shift keying (QPSK) constellations after one-hot encoding function , can be expressed as

$$\begin{aligned} c_1 = 1 &\rightarrow \mathbf{p}_1 = [1, 0, 0, 0] \\ c_2 = -1 &\rightarrow \mathbf{p}_2 = [0, 1, 0, 0] \\ c_3 = 1 &\rightarrow \mathbf{p}_3 = [0, 0, 1, 0] \\ c_4 = -1 &\rightarrow \mathbf{p}_4 = [0, 0, 0, 1] \end{aligned} \quad (10)$$

As Fig. 4 shows the constellation diagrams for QPSK and 16-QAM modulation. Constellation diagram has been widely used in digital modulation design and analysis of signals [26]–[29]. Moreover, the constellation diagram can intuitively display the correlation between the signal structure and various modulation states through the position and distribution of the constellation points [27]. Therefore, we can achieve better signal equalization performance by using the positional relationship information of constellation points combined with the classification structure based the DL method.

Generally, when inputs are not unit vectors, the mapping function can be expressed as

$$\mathbf{s} = \varepsilon_o(\mathbf{q}) = \sum_{i=1}^{|\mathcal{C}|} c_i [\mathbf{q}]_i. \quad (11)$$

The above equation holds for scalar symbols. For the the SISO model, the vector  $\mathbf{q} \in \{0, 1\}^{|\mathcal{C}| \times 2N}$  of  $2N$  symbols from finite

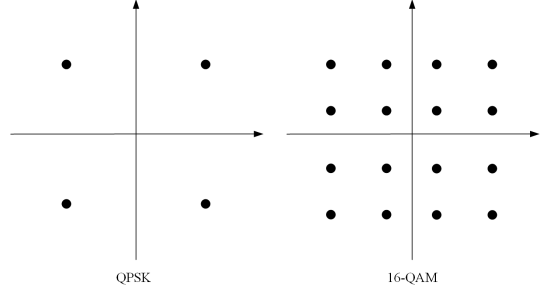


Fig. 4: Constellation diagrams of QPSK and 16-QAM modulation formats.

constellation is mapped to  $\mathbf{s} \in \hat{\mathbb{C}}^{2K}$ .

#### B. Fully Connected Layer

The ML equalizer involves an exhaustive search and is the optimal equalizer in the sense of minimum joint probability of error for detecting all the symbols simultaneously [21]. Unfortunately, computational complexity of ML will increase exponentially with the increase of sub-carriers  $N$ . Especially, the number of OFDM signal sub-carriers transmitted in the UWA channel is relatively large, the ML algorithm is generally difficult to achieve in the UWA environment with a traditional way. Therefore, ML is usually replaced by sub-optimal equalizers such as MMSE in practice. The ML algorithm can be expressed as

$$\hat{\mathbf{s}} = \arg \min_{s \in \hat{\mathbb{C}}^{2N}} \|\mathbf{y} - \mathbf{H}\mathbf{s}\|. \quad (12)$$

We use the deep network to unfold the ML algorithm to achieve a balance between the computational complexity and the accuracy in the frequency domain equalizer.

From Eq. (4), it can be seen that the relationship between  $\mathbf{y}$  and  $\mathbf{H}$  is defined as follows

$$\mathbf{H}^T \mathbf{y} = \mathbf{H}^T \mathbf{H} \mathbf{s} + \mathbf{H}^T \mathbf{z}. \quad (13)$$

The gradient steepest descent method is used to find out the global minimum point. Therefore, the whole iterative algorithm of the network can be formulated as

$$\mathbf{d}_m = \mathbf{W}_m \begin{bmatrix} \hat{\mathbf{s}}_m \\ \lambda_{m1} \mathbf{H}^T \mathbf{y} \\ \lambda_{m2} \mathbf{H}^T \mathbf{H} \hat{\mathbf{s}}_m \end{bmatrix} + \mathbf{n}_m, \quad (14)$$

where  $\mathbf{W}_m$  means the weight matrix of the neural network,  $\mathbf{n}_m$  means the bias term, and  $\lambda_{m1}$  and  $\lambda_{m2}$  represent the step size parameters. Some networks implement zero initialization to the initial value  $\hat{\mathbf{s}}_0$ . In this paper,  $\hat{\mathbf{s}}_0$  is assigned the initial value of ZF equalization to further improve the equalization performance of the network. Since the matrix is not necessarily non-singular, the expression of ZF equalization should be written in pseudo-inverse form  $\hat{\mathbf{s}}_0 = (\mathbf{H}^T \mathbf{H})^{-1} \mathbf{H}^T \mathbf{y}$ . The output  $\mathbf{d}_m$  of the fully connected layer needs to be nonlinearly processed by the activation function  $\mathbf{A}_m = \zeta_m(\mathbf{d}_m)$ . The activation function used in each layer of the UDNet is the hyperbolic tangent function  $\tanh$ .

### C. KL Criterion

Traditional signal equalization algorithms generally adopt the minimum MSE criterion, which are difficult to achieve the minimum SER performance. Therefore, we use the characteristics of constellation diagram to design the network structure to get better SER performance. We perform one-hot encoding with constellation diagram by utilizing these position and distribution information of constellation points to obtain the true value as label. Modulation classification is fundamentally regarded as a multi-class decision task [29]. Thus, we consider M-PSK or M-QAM modulation as a  $M$  classification problem. Hence, the proposed network adopts a *softmax* layer based on the classification idea to obtain the predicted value distribution most similar to the true value distribution. The mapping via the *softmax* function to achieve the predicted value of the constellation map after one-hot encoding  $\hat{\mathbf{q}}_m = \text{softmax}(\mathbf{A}_m)$ . Then  $\hat{\mathbf{q}}_m$  via mapping function to obtain  $\hat{\mathbf{s}}_{m+1} = \varepsilon_o(\mathbf{q}_m)$ . During the  $m^{th}$  iteration as Fig. 3 shows, we obtain the  $\hat{\mathbf{s}}_{m+1}$  as input of the  $(m+1)^{th}$  layer network. Moreover, a cross-entropy loss function is employed to find the closest distance between the predicted value  $\hat{\mathbf{q}}$  and the true value  $\mathbf{q}_e$ . The loss function can be expressed

$$\text{loss}(D_\vartheta(\mathbf{y}, \mathbf{H})) = - \sum_{m=1}^M \mathbf{q}_e \log(m)(\hat{\mathbf{q}}). \quad (15)$$

The total number of layers of UDNet is  $M$ . We use  $\mathbf{D}_\vartheta(\mathbf{y}, \mathbf{H})$  to denote the complete structure of the UDNet. The input of the network is  $\mathbf{y}$  and  $\mathbf{H}$ .  $\vartheta$  represents the training parameters used in the network. We denote  $\hat{\mathbf{q}}$  as the output of the proposed network.

### D. Sliding Structure of OFDM Signal

The number of OFDM sub-carriers  $N$  in UWA communication is relatively large. As  $N$  increases, the channel matrix becomes larger. The complete signal matrix calculation will take up a very large amount of memory and bring in a burden

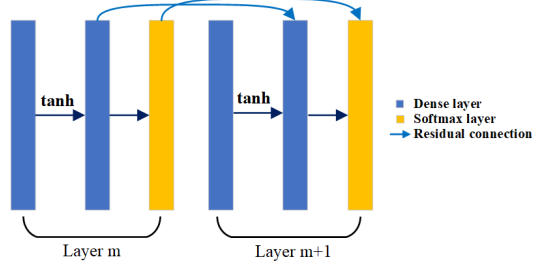


Fig. 5: The structure of residual connection.

of calculation. Although all the elements in the time-varying channel matrix are non-zero, the ICI of the  $m^{th}$  subcarrier working on the  $k^{th}$  sub-carrier in the channel matrix will decay rapidly when  $|k - m|$  is large. Thus, the ICI is considered approximate zero when it is extremely small, the channel matrix can be simplified in a quasi-band shape [13], [30]. The heatmap of the doubly-spread channel in Fig. 2(a) also illustrates the rationality for this simplification. Let the matrix  $\mathbf{H}$  be split into sliding blocks represented as

$$\mathbf{H} = \begin{bmatrix} \phi_1 & & & \\ & \phi_2 & & \\ & & \ddots & \\ & & & \phi_J \end{bmatrix}, \quad (16)$$

where  $J$  means the number of sliding blocks, and  $\phi_j$  represents the  $j^{th}$  sliding block of  $\mathbf{H}$ . Meanwhile, the received signal  $\mathbf{y}$ , the estimated value of the transmitted signal  $\hat{\mathbf{s}}$  can be expressed as

$$\mathbf{y} = [\Gamma_1 \ \Gamma_2 \ \cdots \ \Gamma_J], \quad (17)$$

$$\hat{\mathbf{s}} = [\Upsilon_1 \ \Upsilon_2 \ \cdots \ \Upsilon_J], \quad (18)$$

where  $\Gamma_j$  and  $\Upsilon_j$  represents the  $j^{th}$  sliding block of  $\mathbf{y}$  and  $\hat{\mathbf{s}}$ , respectively. Block-like segmented sliding processing is performed on the input signals  $\mathbf{H}$ ,  $\mathbf{y}$  and  $\hat{\mathbf{s}}$ , thereby reducing the problem of insufficient computing resources and memory. Therefore, we get the network output with sliding blocks as

$$\hat{\mathbf{q}} = [\Omega_1 \ \Omega_2 \ \cdots \ \Omega_J], \quad (19)$$

where  $\Omega_j$  represents the  $j^{th}$  sliding block of  $\hat{\mathbf{q}}$ .

In order to avoid vanishing gradient problem in the proposed network, as shown in Fig. 5, we consider more cross-layer residual connections to solve the problem of vanishing gradient.

## IV. EXPERIMENTAL RESULTS

### A. Training Parameter Settings

In this section, we introduce the detailed parameters of the network. We utilize tensorflow architecture and python3.6 for training. Table I lists the system parameters of UDNet training. The network is trained using the adaptive moment estimation (Adam) gradient descent method. The total layer number of UDNet is  $M = 22$ . The initial learning rate is set to 0.001

TABLE I: Summary of System Parameters for UDNet Based Doubly-spread UWA-OFDM

Parameters	Value
UWA modulation scheme	OFDM with QPSK and 16-QAM
NO. of sub-carriers	512/1024/2048
Channel length	120 taps
sliding block of $\mathbf{H}$ size	32*32
sliding block of $\mathbf{y}$ , $\mathbf{s}$ and $\mathbf{q}$ size	32*1
Training SNR	25dB
Testing SNR	10/15/20/25/30/35dB
Optimizer	Adam
Total layer number	22
Learning rate	0.001
Batch size	2000

with the training batch of UDNet is set to 2000. The channel length is set to 120 taps. The channel matrix is divided into 32 \* 32 size of sliding block and input to the UDNet. In the experiment, the SNR is fixed at 25dB for training. During the test, our network was observed in a SNR of 10-35dB.

The number of sub-carriers of the selected OFDM signal is  $N=512$  by default. Due to the large sub-carrier of the UWA signal and the limitation of computer memory, the algorithms we compared are all processed with sliding structure. The signal modulation method is QPSK and 16-QAM. When we compare the performance of different algorithms, we will use the following naming convention:

**MMSE:** MMSE is the classic algorithm of equalizers.

**DFE:** A decision feedback equalizer (DFE) algorithm.

**SDR:** A decoder based on semidefinite relaxation using efficient interior point solver in [31].

**DetNet:** The detector architecture based DL proposed in [21].

**SCN:** Proposed method in [13], which is a novel equalizer method, combining deep unfolding and sliding structure.

**UDNet:** The equalizer network architecture proposed in this paper.

### B. Training and Testing Dataset

We show the parameters of the UWA doubly-spread channel impulse response (CIR) dataset in Table II. Our dataset contains simulated and measured UWA CIRs which are used in short-distance and shallow water communication scenarios. Fig. 6 shows the CIRs of three underwater channels. The doubly-spread channel matrices that generated from the raw CIRs were measured at Norway—Oslofjord (NOF) [32]. The dataset generated by NOF of 75% is used for offline training of UDNet, and the remaining 25% is used for online testing. And other CIRs measured under different environments are considered for on-line testing. The raw CIRs were measured at Norway—Continental Shelf (NCS) [32] and we create a part of data by BELLHOP (SIM-B) which is a well-known UWA channel simulation method [33], [34].

### C. SER Performance under Different Channels

In the following experiments of different channels, we assume that the CSI is perfect.

1) *Quasi-Static Channel:* In the scenario of quasi-static channel, channel is constant within an OFDM symbol. In this case, Eq. (2) can be simplified as

$$y(n) = \sum_{n=0}^N \sum_{l=0}^{L-1} h(l)s(n-l) + z(n). \quad (20)$$

Frequency domain channel matrix  $\mathbf{H}$  has non-zero value only on the diagonal. Meanwhile, the influence of the Doppler frequency shift of  $\mathbf{H}$  can be ignored. Fig. 7 shows the UDNet performs similar to the traditional methods as MMSE and SDR. In the face of simple quasi-state scenarios, the advantages of complex networks are not highlighted but Classical methods perform well.

2) *Doubly-Spread Channel:* In the scenario of doubly-spread channel, channel varies within an OFDM symbol as shown in Eq. (2). Most of the energy in the frequency domain channel matrix  $\mathbf{H}$  is concentrated in its banded area. Furthermore, we need to pay attention to the impact of Doppler shift of  $\mathbf{H}$ . Fig. 8 shows the test results in the measured NOF channel. It can be seen that the performance of UDNet is better than other methods between wide range of SNR. However, when SNR is high, the downward trend of the UDNet curve slows down. This is due to the quasi-band processing of the channel matrix, ignoring some non-zero values, resulting in limited improvement of equalization accuracy under high SNR. From Fig. 9 and Fig. 10, we show the generalization of UDNet in different channels including NCS and SIM. For NCS channels, in the SNR of 0-35dB, UDNet consistently outperforms other algorithms. For the SIM channel, UDNet shows better performance than other algorithms in high SNR, meanwhile, it performs only has a gap with the DFE algorithm in low SNR. Comparing the experimental results of the three different channels, it is confirmed that as shown in Fig. 4, the doubly-spread channel dataset generated by NCS is the most complicated. Simultaneously, UDNet shows superior performance over complex channels. As a result, we can see that the other algorithms which have weaker ability to deal with variable channels and the UDNet is able to generalize over the changeable Channel characteristics. Fig. 11 presents the experimental results over an high order constellation of 16-QAM. For high order modulation constellations, the SDR algorithm will be limited [21]. Meanwhile, it is observed in our experiment that SCN will not converge over 16-QAM modulated signal. From Fig. 11, We can know the UDNet performs better than DFE and DetNet for the 16-QAM constellation. These results show that the strategy of using probability as soft information and employing KL criterion to get the maximum similarity makes the proposed network more adaptable for high order constellation.

### D. Impact of Clipping and Filtering Distortion

The high peak-to-average power ratio (PAPR) which is a significant shortcoming of OFDM, can be reduced by clipping. However clipping will introduce non-linear noise and the

TABLE II: PARAMETERS OF THE TEST CHANNELS

Paras	NOF	NCS	SIM
Environment	Fjord	Shelf	Default
Range	750m	540m	500m-8000m
Water depth	10m	80m	100m
Transmitter depl	Bottom	Bottom	Suspended
Receiver depl	Bottom	Bottom	Suspended
Doppler coverage	7.8Hz	31.4Hz	Uncalculated
Type	SISO	SISO	SISO

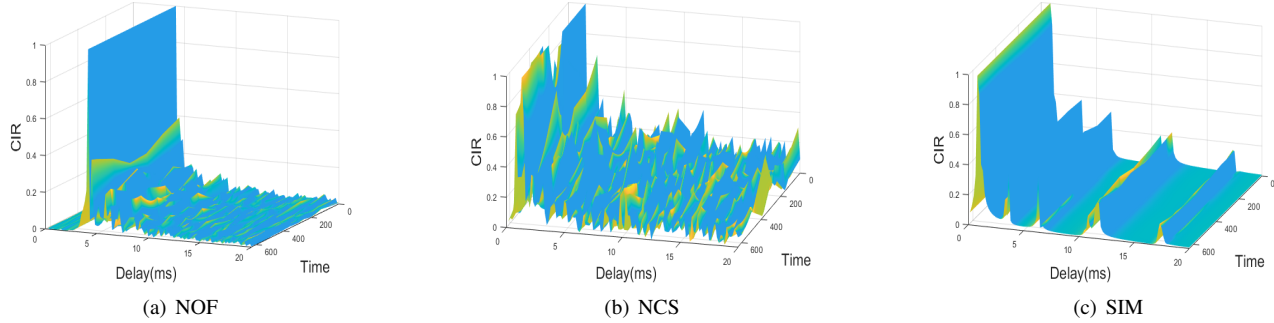


Fig. 6: Impulse Response of Three UWA Channels.

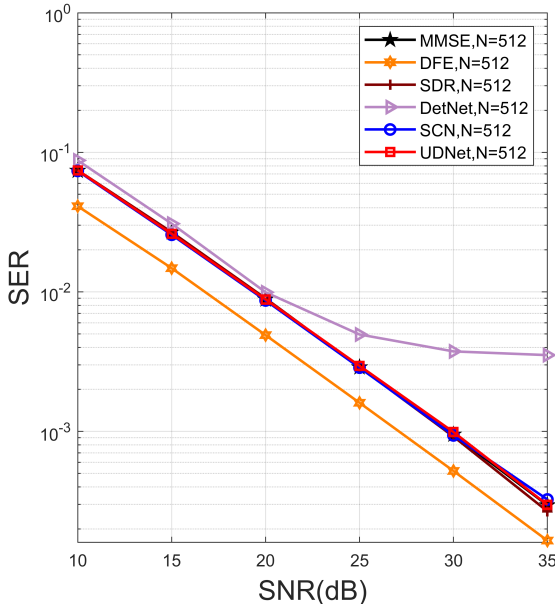


Fig. 7: Comparison of different algorithms over quasi-static channel using QPSK modulation.

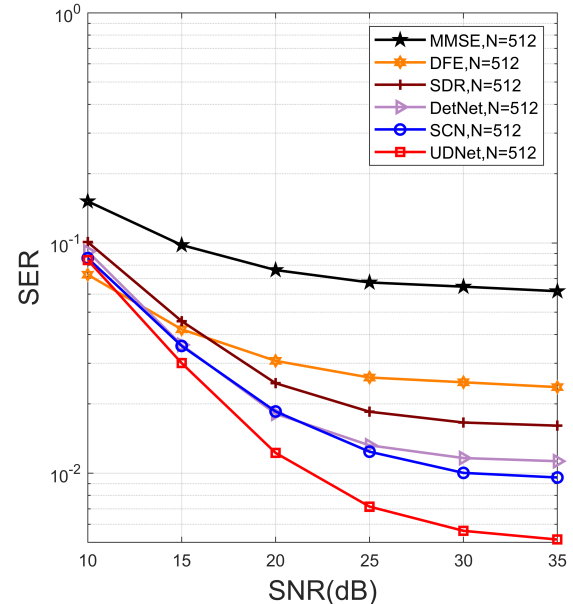


Fig. 8: Comparison of different algorithms over NOF channel using QPSK modulation.

received data may be badly distorted. We set the clipping ratio to OFDM signal as 1 [14]. Hence, the clipped signal can be expressed as

$$c(n) = \begin{cases} c(n), & \text{if } |c(n)| \leq A \\ Ae^{j\phi(n)}, & \text{otherwise} \end{cases}, \quad (21)$$

where  $A$  is the limiting threshold,  $c(n)$  is the received signal, and  $\phi(n)$  is the phase of  $c(n)$ . Fig. 12 shows the comparation of UDNet and other algorithms under clipping and filtering distortion. As we can observe, all methods have a decay with SER performance under clipping noise setting. Simultaneously, in almost covering 10-35dB SNR, Fig. 12 shows that the UDNet method outperforms the other methods. This result

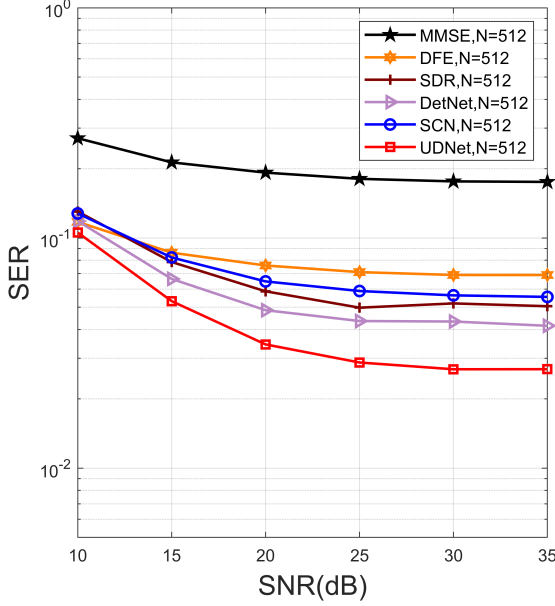


Fig. 9: Comparison of different algorithms over NCS channel using QPSK modulation.

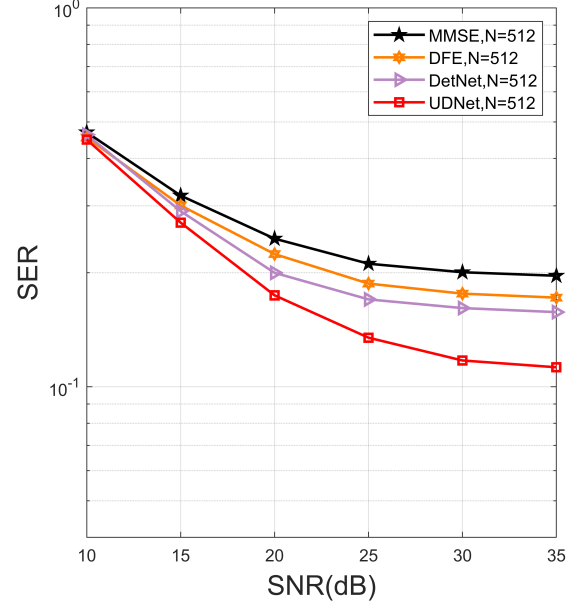


Fig. 11: Comparison of different algorithms over NOF channel using 16-QAM modulation.

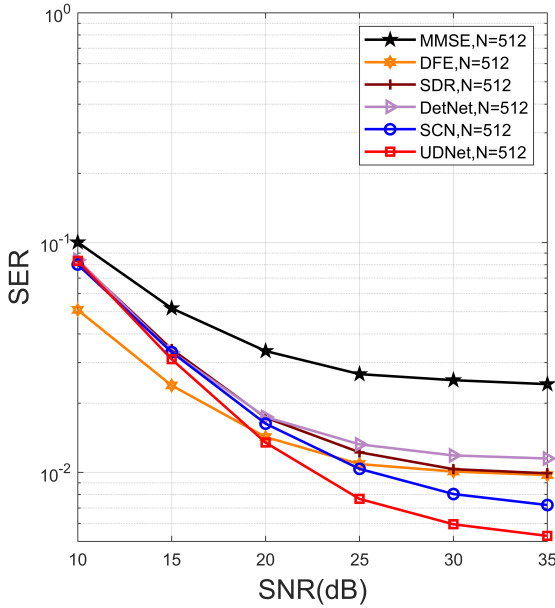


Fig. 10: Comparison of different algorithms over SIM channel using QPSK modulation.

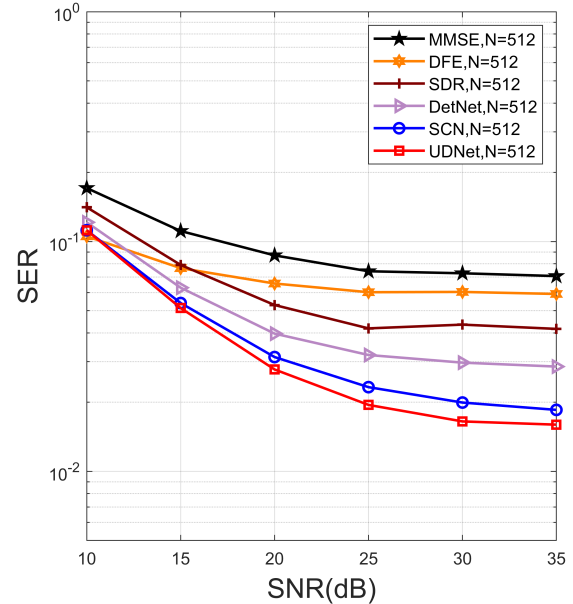


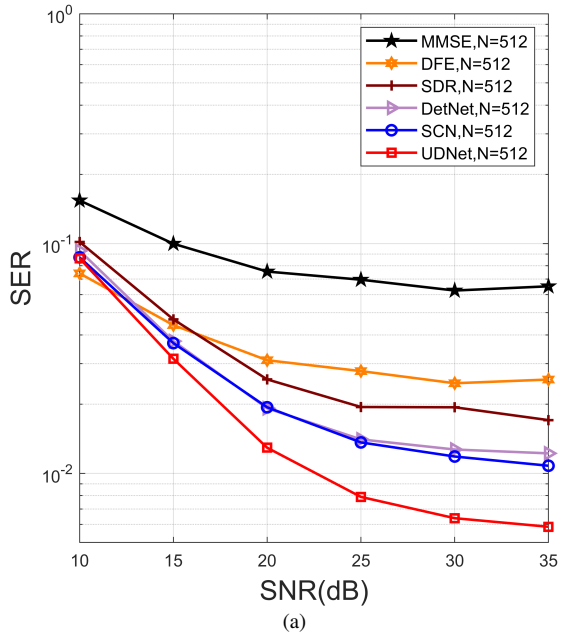
Fig. 12: Comparison of different algorithms under clipping over NOF channel using QPSK modulation.

proves the UDNet method is more robust with the nonlinear clipping noise.

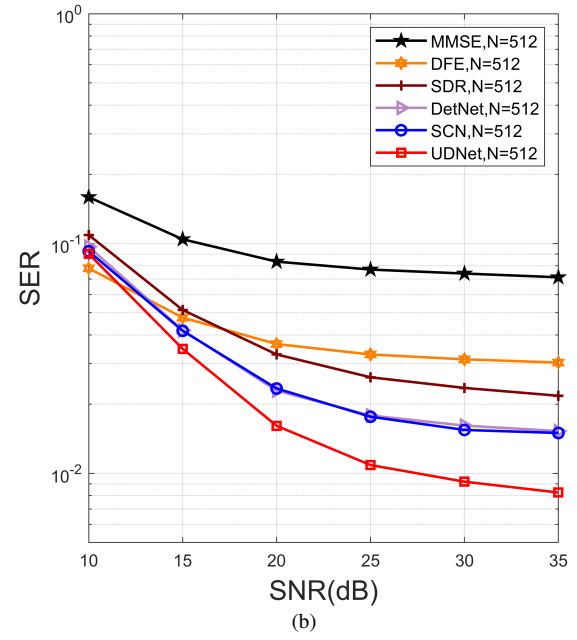
#### E. SER Performance under Imperfect CSI

It is known that acquire perfect CSI in actual communication system is almost impossible. Therefore, we test the robustness of these equalization algorithms with imperfect CSI to learn the performance of these algorithms in practice. We

set the mean value  $\bar{u}$  of random error matrix  $\mathbf{U}$  with as 1. And standard deviation  $\sigma$  of random error matrix  $\mathbf{U}$  is 0.1 and 0.2, respectively. The  $\sigma$  represents the degree to which  $\mathbf{UH}$  deviates from  $\mathbf{H}$ . Fig. 13 shows that as the more  $\mathbf{UH}$  deviates from  $\mathbf{H}$ , CSI more imperfect and the performance of all equalizer algorithms decreases. However, UDNet still performs better than other methods in the varying degrees



(a)



(b)

Fig. 13: Comparison of different algorithms over NOF channel using QPSK modulation when CSI is imperfect: a)  $\bar{u} = 1$ ,  $\sigma = 0.1$ . b)  $\bar{u} = 1$ ,  $\sigma = 0.2$ .

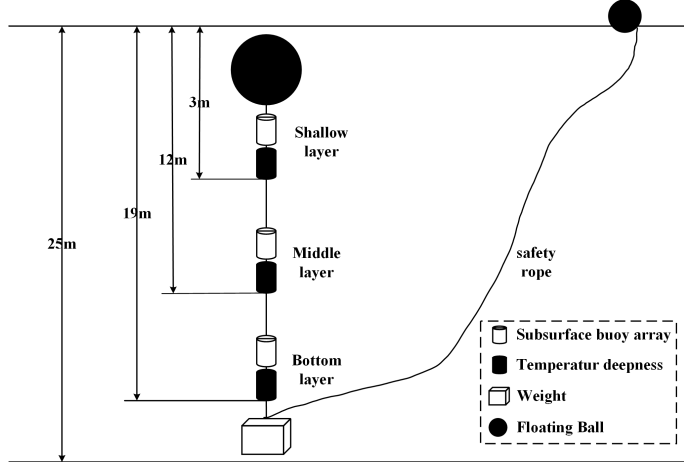


Fig. 14: Bottom-mounted submersible offshore noise acquisition system off Yangjiang nanpeng island.

of imperfect CSI. This is because traditional algorithms rely more on correct channel estimation, but the channel estimation error introduced by imperfect CSI will affect its accuracy. And the DL based methods have better robustness, especially where utilize probability as the output of soft information like UDNet.

#### F. SER Performance under Collected Offshore Background Noise

The additive noise added in previous experiments is AWGN. In this section, we test the proposed algorithm with commun-

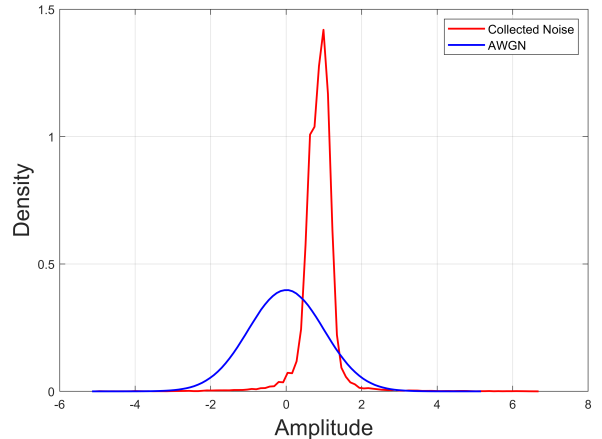


Fig. 15: Comparison of the collected noise and AWGN.

nications signals corrupted by truly collected offshore background noise. The marine noise of the UWA channel is a kind of non-white Gaussian noise composed of sounds from turbulence, shipping, wind and waves, and thermal noise. In the Yangjiang Nanpeng Island offshore wind farm, we use a self-contained acoustic recorder to collect offshore background noise, and the collection lasted for two days. Fig. 14 shows the noise collecting system which adopts a bottom-mounted diving subsurface buoy. The subsurface buoy arrays are placed in the shallow layer 3 meters away from the water surface, middle layer 12 meters away from the water surface, and bottom layer 15 meters away from the water surface, respectively.

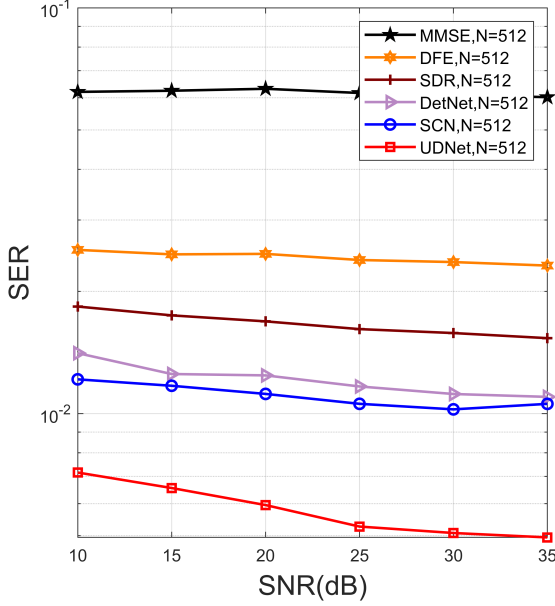


Fig. 16: Comparison of anti-noise performance of different algorithms over NOF channel using QPSK modulation.

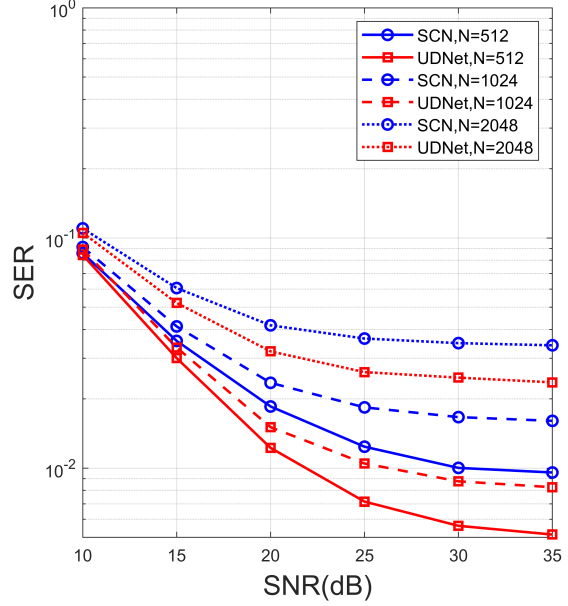


Fig. 18: Comparison of SER performance of SCN and UDNet over NOF channel using QPSK modulation when numbers of sub-carriers are changeable.

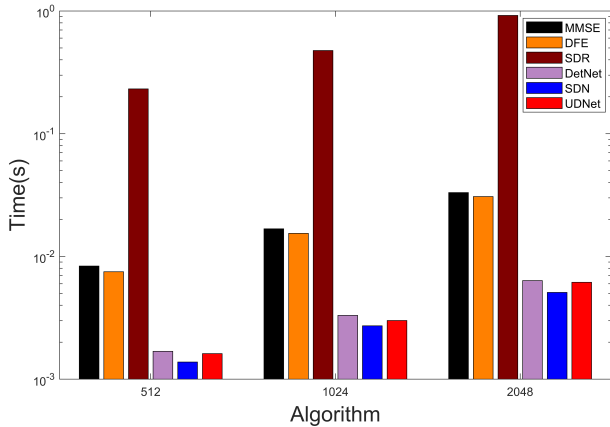


Fig. 17: Comparison of the calculation time of different algorithms over NOF channel using QPSK modulation.

The floating ball keeps the subsurface buoy suspended, and a weight is added to the bottom of the device to keep the whole device vertical.

It can be seen from Fig. 15 that the probability density function of the collected noise, which has a non-zero mean value, differs from AWGN. The NOF channel was probed between 10 and 18 kHz [32]. The collected noise is filtered by a band-pass filter to obtain the processed noise in the same frequency band with NOF. We use the filtered noise as the background noise of the UWA signal for the anti-noise experiment of UDNet. The experimental result are shown in Fig. 16, we can see the SER performance of UDNet is better than other algorithms in the range of 0-35dB SNR. This clearly shows that UDNet has more stable anti-noise

performance. In summary, we take advantage of constellation diagram features for one-hot encoding and take measures of classification structure to make the network more robust to truly offshore background noise. And the result further illustrate the advantages of UDNet in the underwater environment.

#### G. Complexity Analysis

It should be noted, we explored the comparison experiment of complexity on NVIDIA GeForce RTX 3090.

1) *Network Model Complexity*: Table III compares the complexities of the equalizers based deep unfolding parameters including the amount of floating-point multiplication-adds (FLOPs), number of model parameters, model size. The comparison result shows the model complexity of UDNet is between DetNet and SCN. This is because UDNet does not employ the wide neural networks like DetNet, which reduces the amount of calculation. And our network is compared with SCNet, it induces more residual connection structures and a classification structure to improve network performance. Therefore, these added useful structures result in UDNet being more complex than SCN. In conclusion, UDNet has tolerable complexity.

2) *Impact with Number of sub-carriers*: To further explore the complexity of different algorithms, we conduct the following experiments when number of sub-carriers differs. The average calculation time required by diverse algorithms in the face of different numbers of sub-carriers is shown in Fig. 17. The experimental result shows that the computational complexity of UDNet is less than other algorithms except SCN. The result of this comparison is consistent with the result in Table III. Fig. 18 shows the SER performance of UDNet is

TABLE III: Complexity Analysis For UDNet And Other Methods

Name	Flops	Paras	Memory
DetNet	0.96M	0.47M	2.1MB
SCN	0.39M	0.20M	0.85MB
UDNet	0.65M	0.33M	1.5MB

better than SCN when the number of sub-carriers is  $N=512$ , 1024, and 2048. Therefore, it can be concluded that UDNet achieves a balance of computational complexity and accuracy, and also it is more generally applicable.

## V. CONCLUSION

In this paper, we proposed a deep architecture UDNet to equalize OFDM signal transmitted over UWA doubly-spread channel. A classification structure and more cross-layer residual connections are employed for the equalizer. We built several UWA experiment channels that are as realistic as possible. Experimental results indicated that the proposed UDNet outperforms classical equalization algorithms and deep unfolding equalizers such as DetNet and SCN with acceptable algorithm complexity. And our network has a certain generalization in these experiment channels. Meanwhile, UDNet possessed comparatively better robustness against perfect or imperfect CSI. Apart from this, our network is proved that performs better in true offshore background noise environment.

## REFERENCES

- [1] L. Liu, S. Zhou, and J. Cui, "Prospects and problems of wireless communications for underwater sensor networks," *Wireless Commun. Mobile Comput.*, vol. 8, no. 8, pp. 977–994, Oct. 2008.
- [2] J. Catipovic, A. Baggeroer, K. V on der Heydt, and D. Koelsch, "Design and performance analysis of a digital acoustic telemetry system for the short range underwater channel," *IEEE J. Oceanic Eng.*, vol. 9, no. 4, pp. 242–252, Oct. 1984.
- [3] M. Stojanovic and J. Preisig, "Underwater acoustic communication channels: Propagation models and statistical characterization," *IEEE Commun. Mag.*, vol. 47, no. 1, pp. 84–89, Jan. 2009.
- [4] S. Daoud and A. Ghayeb, "Using Resampling to Combat Doppler Scaling in UWA Channels With Single-Carrier Modulation and Frequency-Domain Equalization," *IEEE Trans. Veh. Technol.*, vol. 65, no. 3, pp. 1261–1270, March. 2016.
- [5] J. Tao, "DFT-Precoded MIMO OFDM Underwater Acoustic Communications," *IEEE J. Oceanic Eng.*, vol. 43, no. 3, pp. 805–819, July 2018.
- [6] J. Catipovic, M. Johnson, and D. Adam, "Noise cancelling performance of an adaptive receiver for underwater communications," *Proc. Symp. Auton. Underwater Veh. Technol.*, Jul. 1994, pp. 171–178.
- [7] D. B. Kilfoyle and A. B. Baggeroer, "The state of the art in underwater acoustic telemetry," *IEEE J. Oceanic Eng.*, vol. 25, no. 1, pp. 4–27, Jan. 2000.
- [8] M. T. Altabbaa, "Double focusing: A new sparse channel estimation algorithm for doubly selective SFBC-OFDM-based underwater acoustic systems," *IEEE Wireless Commun. Lett.*, vol. 9, no. 12, pp. 2040–2044, Dec. 2020.
- [9] B. Li, S. Zhou, M. Stojanovic, L. Freitag and P. Willett, "Multicarrier Communication Over Underwater Acoustic Channels With Nonuniform Doppler Shifts," *IEEE J. Oceanic Eng.*, vol. 33, no. 2, pp. 198–209, Apr. 2008.
- [10] E. Panayirci, M. T. Altabbaa and H. V. Poor, "Channel Estimation and Equalization for Alamouti SF-Coded OFDM-UWA Communications," *IEEE Trans. Veh. Technol.*, vol. 70, no. 2, pp. 1709–1723, Feb. 2021.
- [11] Z. An, J. Wang and S. Huang, "MMSE-based equalization and ICI mitigation scheme for OFDM system over doubly selective channels," *IEEE Int. Symp. Broadband Multimedia Syst. Broadcast.*, 2014, pp. 1–4.
- [12] B. Li, S. Zhou, M. Stojanovic, L. Freitag and P. Willett, "Multicarrier Communication Over Underwater Acoustic Channels With Nonuniform Doppler Shifts," *IEEE J. Oceanic Eng.*, vol. 33, no. 2, pp. 198–209, April 2008.
- [13] Q. Huang, C. Zhao, M. Jiang, X. Li and J. Liang, "A Novel OFDM Equalizer for Large Doppler Shift Channel through Deep Learning," *IEEE 90th Veh. Technol. Conf.*, pp. 1–5, 2019.
- [14] H. Ye, G. Y. Li and B. Juang, "Power of Deep Learning for Channel Estimation and Signal Detection in OFDM Systems," *IEEE Wireless Commun. Lett.*, vol. 7, no. 1, pp. 114–117, Feb. 2018.
- [15] X. Gao, S. Jin, C. Wen and G. Y. Li, "ComNet: Combination of Deep Learning and Expert Knowledge in OFDM Receivers," *IEEE Commun. Lett.*, vol. 22, no. 12, pp. 2627–2630, Dec. 2018.
- [16] Y. Zhang et al., "Deep Learning Based Single Carrier Communications Over Time-Varying Underwater Acoustic Channel," *IEEE Access*, vol. 7, pp. 38420–38430, 2019.
- [17] J. Liu, F. Ji, H. Zhao, J. Li and M. Wen, "CNN-Based Underwater Acoustic OFDM Communications over Doubly-Selective Channels," *IEEE 94th Veh. Technol. Conf.*, 2021, pp. 01–06.
- [18] X. Ji, J. Wang, Y. Li, Q. Sun and C. Xu, "Modulation recognition in maritime multipath channels: A blind equalization-aided deep learning approach," *China Commun.*, vol. 17, no. 3, pp. 12–25, March 2020.
- [19] T. Koike-Akino, Y. Wang, D. S. Millar, K. Kojima and K. Parsons, "Neural Turbo Equalization: Deep Learning for Fiber-Optic Nonlinearity Compensation," *J. Lightw. Technol.*, vol. 38, no. 11, pp. 3059–3066, 1 June 1, 2020.
- [20] Hershey J R, Roux J L and Weninger F. Deep Unfolding: Model-Based Inspiration of Novel Deep Architectures[J]. *Computer Science*, 2014.
- [21] N. Samuel, T. Diskin and A. Wiesel, "Learning to Detect," *IEEE Trans. Signal Process.*, vol. 67, no. 10, pp. 2554–2564, May. 2019.
- [22] Z. Liu and T. C. Yang, "On Overhead Reduction in Time-Reversed OFDM Underwater Acoustic Communications," *IEEE J. Oceanic Eng.*, vol. 39, no. 4, pp. 788–800, Oct. 2014.
- [23] Zheng Y. R, Chengshan Xiao, Yang T. C, Wen-Bin Yang, "Frequency Domain Channel Estimation and Equalization for Single Carrier Underwater Acoustic Communications" *IEEE Conf. Oceans*, 2007.
- [24] T. Ebihara and K. Mizutani, "Underwater Acoustic Communication With an Orthogonal Signal Division Multiplexing Scheme in Doubly Spread Channels," *IEEE J. Oceanic Eng.*, vol. 39, no. 1, pp. 47–58, Jan. 2014.
- [25] P. K. Rajasekaran, N. Satyanarayana and M. D. Srinath, "Optimum Linear Estimation of Stochastic Signals in the Presence of Multiplicative Noise," *IEEE Trans. Aerosp. Electron. Syst.*, vol. AES-7, no. 3, pp. 462–468, May. 1971.
- [26] G. Jajoo, Y. Kumar and S. K. Yadav, "Blind Signal PSK/QAM Recognition Using Clustering Analysis of Constellation Signature in Flat Fading Channel," *IEEE Commun. Lett.*, vol. 23, no. 10, pp. 1853–1856, Oct. 2019.
- [27] Y. Kumar, M. Sheoran, G. Jajoo and S. K. Yadav, "Automatic Modulation Classification based on Constellation Density using Deep Learning," *IEEE Commun. Lett.*, vol. 24, no. 6, pp. 1275–1278, June 2020.
- [28] F. Wang, Y. Wang and X. Chen, "Graphic Constellations and DBN Based Automatic Modulation Classification," in *Proc. 2017 IEEE 85th Veh. Technol. Conf. (VTC Spring)*, Sydney, NSW, 2017, pp. 1–5.
- [29] V. -S. Doan, T. Huynh-The, C. -H. Hua, Q. -V. Pham and D. -S. Kim, "Learning Constellation Map with Deep CNN for Accurate Modulation Recognition," *IEEE Global Commun. Conf.*, pp. 1–6, 2020.
- [30] W. G. Jeon, K. H. Chang, and Y. S. Cho, "An equalization technique for orthogonal frequency-division multiplexing systems in time-variant multipath channels," *IEEE Trans. Commun.*, vol. 47, no. 1, pp. 27–32, 1999.
- [31] Z. Q. Luo, W. K. Ma, A. M. So, Y. Y. e, and S. Zhang, "Semidefinite relaxation of quadratic optimization problems," *IEEE Signal Process. Mag.*, vol. 27, no. 3, pp. 20–34, May. 2010.
- [32] P. A. van Walree, F. Socheleau, R. Otnes and T. Jenserud, "The Watermark Benchmark for Underwater Acoustic Modulation Schemes," *IEEE J. Oceanic Eng.*, vol. 42, no. 4, pp. 1007–1018, Oct. 2017.
- [33] H. Zhao, F. Ji, M. Wen, H. Yu and Q. Guan, "Multi-Task Learning Based Underwater Acoustic OFDM Communications," *IEEE Int. Conf. Signal Process. Commun. Comput.*, 2021, pp. 1–5.
- [34] P. Qarabaqi and M. Stojanovic, "Statistical Characterization and Computationally Efficient Modeling of a Class of Underwater Acoustic Communication Channels," *IEEE J. Oceanic Eng.*, vol. 38, no. 4, pp. 701–717, Oct. 2013.